LAWRENCE
LIVERMORE
NATIONAL
LABORATORY

UCRL-JRNL-218429

Evidence of gating in hundred nanometer diameter pores: an experimental and theoretical study

S. E. Letant, C. M. Schaldach, M. R. Johnson, A. Sawvel, W. L. Bourcier, W. D. Wilson

January 26, 2006

Small

Evidence of gating in hundred nanometer diameter pores: an experimental and theoretical study

Sonia E. Létant,[†,*] Charlene M. Schaldach,[†] Mackenzie R. Johnson,[‡] April Sawvel,[‡] William L. Bourcier,[‡] W. D. Wilson[†]

Chemistry and Materials Science Directorate and Energy and Environment Directorate, Lawrence Livermore National Laboratory, 7000 East Avenue, Livermore, CA 94550.

ABSTRACT

We report on the observation of an unexpected gating mechanism at the 100 nm scale on track-etched polycarbonate membranes. Transport measurements of methyl viologen performed by absorption spectroscopy under various pH conditions demonstrated that perfect gating was achieved for 100 nm diameter pores at pH 2, while the positively charged molecular ions moved through the membrane according to diffusion laws at pH 5. An oppositely charged molecular ion, naphthalene disulfonate, in the same membrane, showed the opposite trend: diffusion of the negative ion at pH 2 and perfect gating at pH 5. The influence of parameters such as ionic strength and membrane surface coating were also investigated. A theoretical study of the system shows that at this larger length scale the magnitude of the electric field in the vicinity of the pores is too small to account for the experimental observations, rather, it is the surface trapping of the mobile ion (Cl^- or Na^+) which gives rise to the gating phenomena. This surprising effect might have potential applications for high-throughput separation of large molecules and bio-organisms.

* Corresponding author
† Chemistry and Materials Science Directorate
‡ Energy and Environment Directorate

Introduction

Gaining the ability to selectively control the passage of molecules in artificial pores via physical or chemical stimulation will be essential for the development of the next generation of sensor and separation platforms. Nature achieves this challenge on a daily basis to control the transport of ions in and out of cells. Ion channel proteins embedded in the cellular membrane are indeed able to selectively pump ions against concentration gradients.[1] Although the mechanism is not perfectly understood, it is believed that the extreme selectivity of the ion channels is generated by a combination of size selection and chemical affinity. Various approaches have been taken toward the formation of artificial ion channels, the goal being to trigger the opening or closing of the channel gate to the passage of specific chemical species with physical parameters such as light, heat, and electrical impulses, or chemical parameters such as temperature, ionic strength, and pH. Selective transport and gating (prevention of the molecular ion from diffusing to the bottom of the membrane pore) have both been demonstrated on artificial pores at the nanometer scale.[2-10] One example is the use of antibody-functionalized gold-coated nanopores for enantiomeric drug separation.[11] Another example is the rectifying effect observed on asymmetric polycarbonate nano-channels.[12-14] It is important to stress that these effects were always observed when the channel dimensions matched the molecule or ion dimensions, typically the 1 nm scale, which dramatically limits the throughput of this approach for separation applications.

In this letter, we report on the observation of a perfect gating mechanism occurring at the 100 nm scale. This effect could potentially be used for high-throughput separation of large molecules and bio-organisms.

Experimental

Transport of methyl viologen (see chemical structure in Figure 1) through polycarbonate membranes was studied in aqueous media under various conditions. Commercial track-etched material (Nucleopore, Whatman) with a thickness of 6 μm and a pore density of 4 x 10^8 pores per cm^2 was used in all experiments. Membranes were sandwiched between two silicon rubber gaskets and mounted in a two compartment diffusion cell probing an area of 20 mm^2. All solutions were prepared using deionized water with a resistivity of 18 MΩ and a pH of 5 (referred to as DI water), and methyl viologen (MV^{2+}) dichloride hydrate (98%, Sigma-Aldrich). When pH values below 5 were used, the pH of the solution was adjusted using sulfuric acid. Prior to each diffusion experiment, both compartments were filled with a 1:4 ethanol:water solution by volume in order to wet the pores. After 2 H 30 min, the reservoirs were emptied and filled with the blank background solution to be used as the permeate for the experiment. The blank permeate solution was then re-circulated at a speed of 1.7 mL / min into the quartz flow cell of a UV-vis spectrometer (Varian Inc., Model Cary 100) with a peristaltic pump (VWR Variable Flow Mini-Pump II, Model 3385), and the instrument was zeroed. The feed reservoir was then emptied and filled with the MV^{2+} solution of interest. The absorbance of the permeate solution was continuously collected at 258 nm, the absorbance maximum of MV^{2+}. The experiments were allowed to run until saturation of the absorption signal, which occurs at 0.2 mM MV^{2+} with our experimental setup. After each experiment, the diffusion cell and the gaskets were cleaned by sonication in DI water for 15-18 minutes at 30˚C.

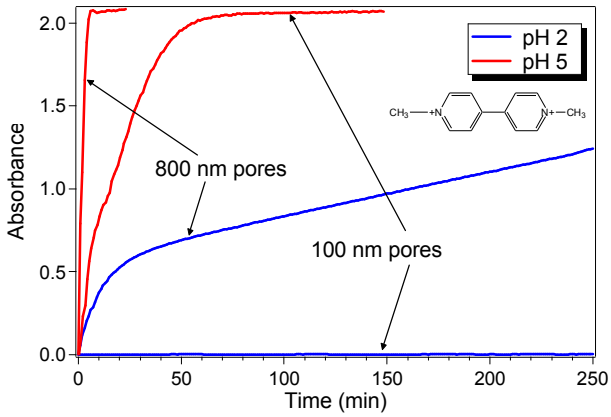

Figure 1. Diffusion of 10 mM MV^{2+} through polycarbonate membranes measured by UV-vis absorbance of the permeate solution at 258 nm. The data is presented for two pore diameters: 800 nm and 100 nm. In both cases, the diffusion of MV^{2+} was measured at pH = 5 (deionized water) and at pH = 2 (deionized water adjusted with sulfuric acid) while other experimental conditions remained unchanged.

The first set of data, presented in Figure 1, shows the rate of diffusion of MV^{2+} ions from a 10 mM solution through polycarbonate membranes with various pore diameters, at pH 5 (DI water) and 2 (DI water adjusted with sulfuric acid). As a control, the MV^{2+} absorbance spectrum was independently measured as a function of time in these solutions and was found to be unaffected by the pH of the solution. Figure 1 shows that while MV^{2+} diffuses normally at pH 5, the transport is reduced or completely stopped at pH 2, depending on the pore diameter. For pore diameters at or below 100 nm (we performed additional experiments at 15nm and 50 nm, data not shown), perfect gating was observed at pH 2. Among possible mechanisms responsible for this gating, steric effects are unlikely, given the small size of the MV^{2+} ion relative to the size of the membrane pore. We believe that electrostatic effects, being of longer range, are worthy of further investigation.

To help identify the mechanism responsible for the observed gating, then, we performed additional experiments on the 100 nm pore diameter material at pH 2. The

gating experiment was repeated with the ionic strength of both the feed and permeate compartments increased to 100 mM by adding KCl (pumped through the system prior to the gating experiment) (see Figure 2a). We also performed the experiment on gold-coated (sputtered) polycarbonate membranes (see Figure 2b). The gating effect was significantly suppressed in both cases for reasons to be discussed below.

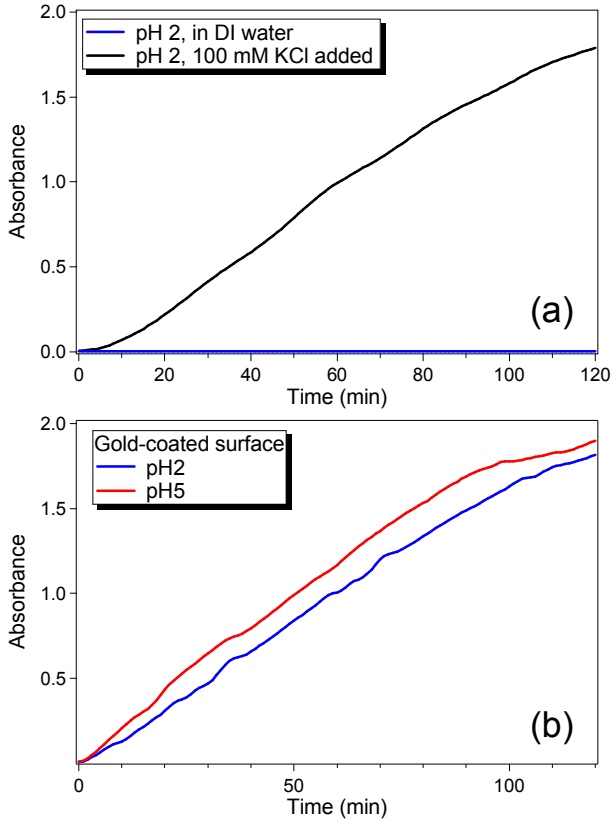

Figure 2. Diffusion of 10 mM MV^{2+} through a 100 nm pore diameter polycarbonate membrane measured by UV-vis absorbance of the permeate solution at 258 nm. (a) Experiment performed at pH 2 without any KCl added (blue line) and with 100 mM KCl added in both feed and permeate solutions (black line). (b) Experiment performed at pH 2 (blue line) and 5 (red line) on a membrane coated with 20 nm of gold by sputtering.

While the transport of MV^{2+} ions can be directly measured by absorbance spectroscopy, the path taken by the chloride ions has to be measured indirectly. A Dionex

DX-120 Ion Chromatograph (IC) fitted with a Dionex IonPac® AS14 Analytical Column was used to analyze the chloride ion concentration in both feed and permeate solutions at the beginning and at the end of the gating experiment run at pH 2 on a 100 nm pore membrane. While the absorption spectrum indicates that gating of MV^{2+} occurred under these experimental conditions (see Fig. 1), the IC results indicate that Cl^- also did not diffuse significantly through the pores (Table 1).

Solution analyzed	Sampling time	Cl^- (mg / L)	Difference (mg / L)	% Cl^- Diffused
Feed	Initial	610.7	44.25	7.2
	Final	566.4		
Permeate	Initial	1.34	0.16	0.36
	Final	1.50		

Table 1. Chloride concentrations of the feed and permeate solutions before and after a 10 mM MV^{2+} diffusion experiment measured by ion chromatography. Gating was accomplished using a 100 nm pore diameter membrane in a pH 2 background solution.

Table 1 also shows that although no noticeable amount of chloride diffuses through the membrane (less than 0.5 %), the chloride content of the feed solution significantly decreases (7.2 % by weight). This disparity is indicative of trapping of chloride ions from the feed solution onto the membrane surface.

In order to rule out the occurrence of a chemical reaction at the membrane surface due to the pH change, or a reaction involving methyl viologen itself, the transport of naphthalene disulfonate (NDS^{2-}) through a 100 nm pore membrane was also investigated at pH 2 and 5 by measuring the absorption at 287 nm. In this case, the counter-ion is Na^+, and the results (not shown) follow the expected opposite trend: diffusion of NDS^{2-} at pH 2 and perfect gating at pH 5. These results indicate that the gating is not a unique

aspect of the chemistry of the methyl viologen ion, and that the existence of gating correlates with a like charge of the membrane surface and the large organic ion.

Computational

Electric fields in the vicinity of nanostructures such as membrane pores used in the experiments presented here are obtained as described in ref [15]. Briefly, the method involves direct summation of charged Debye-Hückel spheres comprising the nanostructural surfaces and has been validated by comparison to analytical solutions for a number of geometries. The motion of charged particles in the vicinity of the pore is treated by solution to the Langevin equation: the stochastic component being diffusion within the pore boundaries (Monte Carlo) and the deterministic component being the velocity induced by the electric field due both to the charged membrane and to that of the surrounding mobile ions. Velocities are obtained from the electrophoretic mobilities, μ_i ($\mu_i=q_i/6\pi\nu R_i$ where q_i is the charge on ion i, R_i its hydrated radius, taken to be 1.4 nm (approximated as spherical) and 0.33 nm[16], respectively, and ν is the viscosity of the fluid, 0.01 poise). Diffusion coefficients for MV^{+2} and Cl^- ions were obtained from the Einstein relation, $D_i=kT/6\pi\nu R_i$, where k and T have their usual meaning. The electric field at a mobile ion due to surrounding mobile ions is found in the Debye-Hückel approximation,

$$\mathbf{E}_i = \sum_j \frac{q_j(1+\kappa r_{ij})\exp(\kappa(r_0 - r_{ij}))}{\varepsilon(1+\kappa r_0)} \frac{\mathbf{r}_{ij}}{r_{ij}^3}$$

where E_i is the electric field at ion i, r_{ij} is the distance between the centers of ion i and ion j, q_j is the charge on ion j, r_o is the radius of ion j, ε is the dielectric constant of water (=78.5), and κ is the inverse Debye length. Summations are taken out to large distances

(~30 nm) because of the long-range nature of this electrostatic interaction in low ionic strength solutions such as employed here.

We seek to determine the mechanism responsible for the gating found in the above experiments. For very small pores (for example, 6.0 nm diameter) in fluids whose salt content (for example, 10 mM KCl) is such that the double layers on opposite sides of the charged membrane overlap (each double layer thickness is ~3.0 nm), ions are not screened by the double layer and hence can experience high enough fields to be repelled or attracted from the pore. Larger pores under the same charging and salt conditions give rise to small electric fields at ions outside the double layer. In the experiments described above, the fluid is de-ionized water which a) has a very long Debye length (very little screening) and b) results in very small surface charge densities.

In Fig. 3, then, we show the results of our calculations of the electrostatic potential and electric field in the vicinity of charged cylindrical pores of diameter 15 nm, 100 nm and 800 nm, respectively. These potentials and fields are deliberately significantly overestimated relative to our experimental conditions: the membrane surface charge density ($\sigma = \frac{\varepsilon\kappa\varphi}{4\pi}$) was obtained from zeta potential measurements on polycarbonate[17,18] in which a significant salt content resulted in significant zeta potential (7 mV in 1 mM KCl). The associated charge density (σ=0.051 $\mu C/cm^2$) provides an upper limit to the surface charge density in our de-ionized water experiments. (Note that this upper limit charge density is quite small.) We maintained this charge density while assuming the inverse Debye length, κ, to be negligible in order to obtain the maximized potentials and electric fields in Fig. 3. The dielectric constant, ε=78.5, appropriate for water is assumed not to vary with distance from the surface. For all three pore sizes, the magnitude of the

electric field in the near vicinity of the mouth of the pore was found to be ~7 x 10^3 volt/cm. The maximum in the z component of the electric field (upward in Fig. 3) along the center line of the pore was found to be ~4.3 x 10^3 volt/cm, ~4.0 x 10^3 volt/cm, and ~1.6x10^3 volt/cm for the 15 nm, 100 nm and 800 nm pores, respectively. As we shall see, these fields are still not large enough to overcome the stochastic effects.

The time required for a MV^{2+} (Cl^-) ion to travel under the influence of an electric field of magnitude 10^3 volt/cm from the pore center to the membrane surface for the 15 nm pore, a distance of 7.5 nm, is ~6.2 x 10^{-6} sec (2.9 x 10^{-6} sec for Cl^-) (using μ_{Cl^-} =2.58x10^{-4} cm^2/volt-sec; μ_{MV2+}=1.21x10^{-4} cm^2/volt-sec; D_{Cl^-}=6.45 x 10^{-6} cm^2/sec; D_{MV2+}=1.51 x 10^{-6} cm^2/sec). For comparison, in this same time interval, the ions would diffuse 74.9 nm and 106.1 nm, respectively, an order of magnitude greater than their migration under the action of the field. At 10^4 volt/cm, these diffusion distances become 23.7 nm and 33.5 nm, respectively, still dominating the effect of the field. At 10^6 volt/cm (test purposes only), however, these diffusion distances become 2.4 nm and 3.4 nm, respectively, indicative of a strong field effect. We performed Langevin calculations on single species, MV^{2+} or Cl^-, diffusing in the presence of the charged membrane to confirm these simple estimates: the membrane field does not prevent the diffusion of either species through the 15 nm pore.

For the 100 nm and 800 nm pore diameters, similar considerations result in diffusion dominating the electric field effects. In these cases, the fields are lower than for the 15 nm pore (see Fig. 3) but the traversal time intervals are longer. The time required for a MV^{2+} (Cl^-) ion to travel under the influence of an electric field of magnitude 10^3 volt/cm from the pore center to the membrane surface for the 800 nm pore, a distance of 400 nm,

is ~3.3 x 10^{-4} sec (1.6 x 10^{-4} sec). In this same time interval, the ions would diffuse 547 nm and 775 nm, respectively, greater than their migration under the action of the field, even for this much over-estimated field magnitude.

The gating of ions in the experiments reported on here is not due to direct electrostatic fields from like-charged membrane surfaces. This is not to say that the membrane charges are irrelevant; at very close distances to a charged surface (a distance to which an ion may jump by diffusion), the field becomes of order ~10^6 volt/cm (the region of dielectric breakdown).

a) 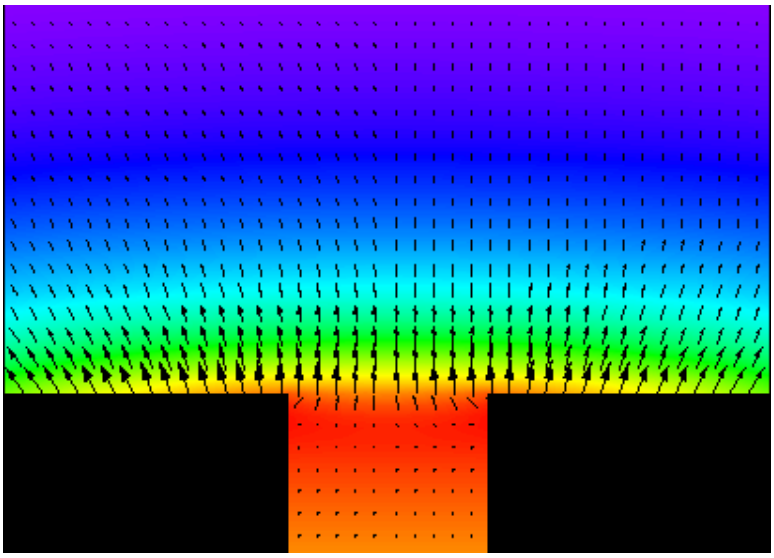

b)

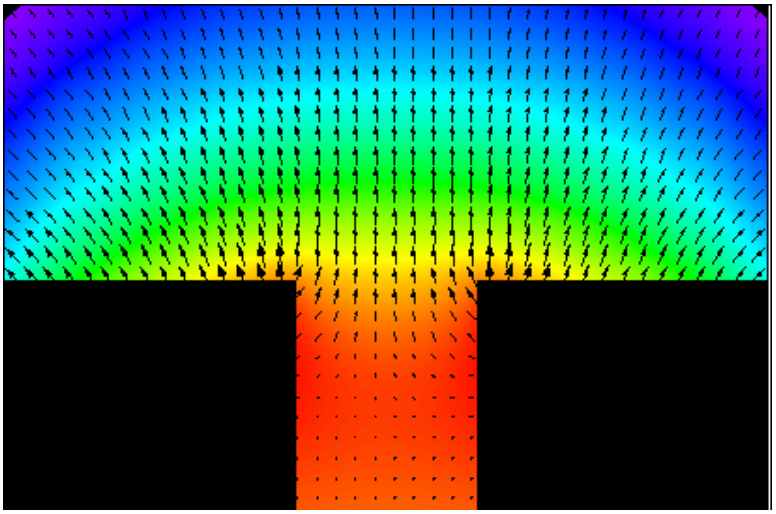

c)

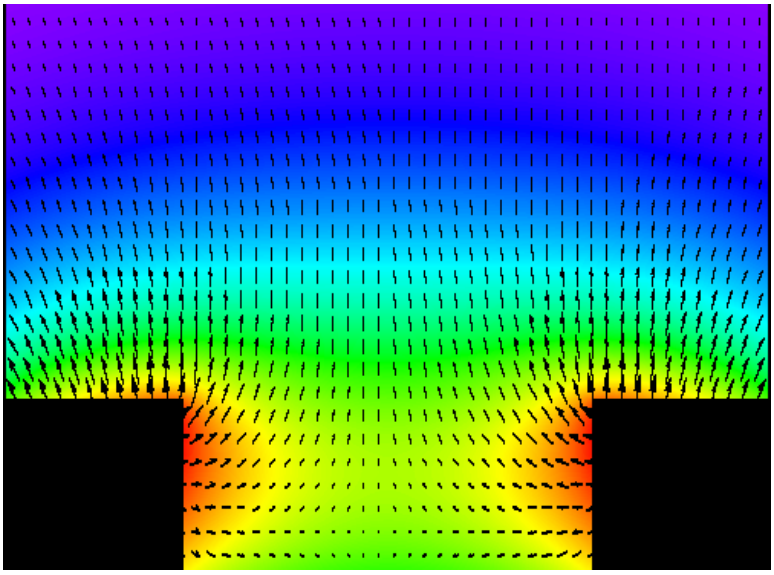

Figure 3. Potential (colored background) and electric field (arrows) in the vicinity of (a) 15 nm, (b) 100 nm and (c) 800 nm pores. For all three pore sizes, the magnitude of the electric field in the near vicinity of the mouth of the pore was found to be ~7 x 10^3 volt/cm. The maximum in the z component of the electric field (upward arrows) along the center line of the pore was found to be ~4.3 x 10^3 volt/cm, ~4.0 x 10^3 volt/cm, and ~1.6x10^3 volt/cm for the 15 nm, 100 nm and 800 nm pores, respectively. These fields are not large enough to overcome the stochastic effects.

An explanation of the gating consistent with our experimental results involves the smaller, more mobile ion driving the system. In the case of the methyl viologen dichloride experiments, the chloride ion is the more mobile of the two dissociated

chemical species, MV^{2+} and Cl^-. When methyl viologen chloride is added to the feed, the Cl^- diffuses more quickly to and through the membrane than the MV^{2+}. (The diffusion coefficient of Cl^- (6.45×10^{-6} cm^2/sec) is ~4 times that of MV^{2+} (1.51×10^{-6} cm^2/sec) in water at room temperature.) At pH=2, we observe gating of MV^{2+}, the MV^{2+} does not permeate through the pore, even when the pore size is too large for the repulsive electric field to affect the motion of the ion except when in its close proximity (see Fig. 3). The membrane is positively charged, however, and, hence, attractive to the more mobile Cl^- ions as they diffuse very close to the charged membrane.

This attraction is significantly greater near the top of the pore as seen in Fig. 3a; the field there is enhanced by virtue of the geometry (see reference [15] for a detailed explanation). This Cl^- attraction increases with decreasing distance to the membrane. Electrostatics-assisted trapping of the Cl^- to the surface (when the ion is in close proximity to the surface), not involving a chemical reaction, is therefore likely, and as mentioned above, is evidenced by the removal of a significant amount of the chloride from the feed. Since we do not find MV^{2+} in the permeate, there is no measured charge separation and therefore the MV^{2+} must be remaining with the trapped chloride (electrostatic attraction) in and above the membrane. Given the large number of chloride ions removed according to the experiments (4.0×10^4 Cl^- ions/nm^2 of surface area), there exist abundant Cl^- ions to bind MV^{2+} and prevent their permeation through the membrane.

Evidence for this mechanism is presented in Fig. 4 where we have plotted the number of MV^{2+} ions (Fig. 4a) and Cl^- ions (Fig. 4b) which have traversed a 52.9 nm (1000 Bohr) plane relative to the top of a 15 nm diameter membrane under various conditions as a

function of time (10^{-10} sec time step). A constant 10 mM concentration of ions is maintained above the membrane pore by replacing those ions that diffuse into the membrane. Rapid diffusion of ions is found under conditions of no surface charge and no electrostatic interactions between ions (labeled "diffusion alone"): ~360 MV^{2+} (~2200 Cl^-) ions cross the plane in $5x10^{-5}$ sec. Next we add the inter-ion electrostatic interactions alone (no membrane surface charge) to obtain the second curves (labeled "inter-ion electrostatics ") in Fig. 4. It is to be noted that the introduction of the attractive interaction of the Cl^- to the less mobile MV^{2+} has slowed down the Cl^- ions so that at $5x10^{-5}$ sec only ~1500 Cl^- ions (as compared to the ~2200 Cl^- ions for diffusion alone) have traversed the plane. Similarly, the inter-ion attraction of the MV^{2+} to the Cl^- speeds up the less mobile MV^{2+} (~540 MV^{2+} ions at $5x10^{-5}$ sec as compared with the 360 MV^{2+} ions) which traverse the plane under diffusion alone.

a)

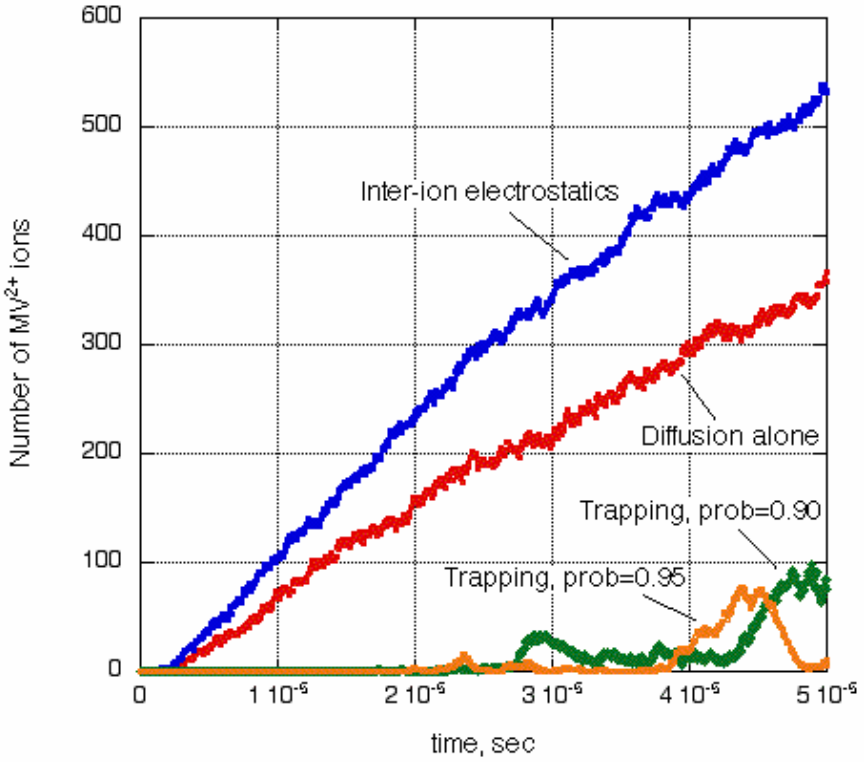

b)

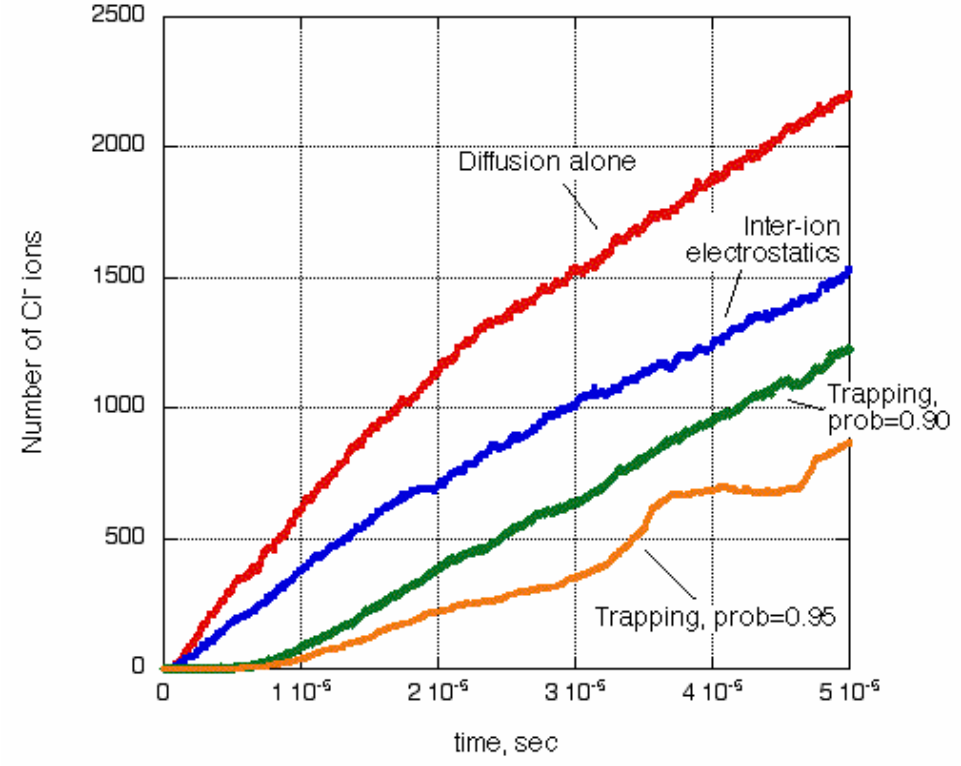

Figure 4. Number of (a) MV^{2+} and (b) Cl- ions crossing a plane 52.9 nm (1000 Bohr) from the entrance (top) of the pore. Rapid diffusion of ions is found under conditions of no surface charge and no electrostatic interactions between ions (labeled "diffusion alone"): ~360 MV^{2+} (~2200 Cl^-) ions cross the plane in $5x10^{-5}$ sec. Adding inter-ion electrostatic interactions alone (no membrane surface charge), we obtain the second curves (labeled "inter-ion electrostatics"). It is to be noted that the introduction of the attractive interaction of the Cl^- to the less mobile MV^{2+} has slowed down the Cl^- ions (Fig. 4a), while speeding up the less mobile MV^{2+} ions (Fig. 4b). Note that the Cl^- ions are reduced to ~1200 ions (~900 ions) for the 0.90 (0.95) trapping probabilities, respectively. Most importantly, the MV^{2+} ions, which are electrostatically attracted to the trapped Cl^- ions, are therefore reduced to less than ~100 ions for the 0.90 trapping probability case, and essentially shut down (<50 ions) for the 0.95 trapping probability case. The more mobile ion determines the fate of the less mobile ion.

The introduction of both polycarbonate surface charge consistent with zeta potential measurements (pH=2) and trapping of the more mobile species to the pore surface is also shown in Fig. 4 (negligible inverse Debye length, as discussed above). The positive surface charge attracts the Cl^- ions when they are near the membrane surface which then become trapped with a probability of 0.90 or 0.95 (see Fig. 4) (and may become de-

trapped with a probability of 0.05 in each case) by an as-yet unspecified mechanism. Only the Cl^- ions are trapped; the MV^{2+} ions are electrostatically repelled by the positive surface charge when they closely approach. It is seen from Fig. 4 that the Cl^- ions are reduced to ~1200 ions (~600 ions) for the 0.90 (0.95) trapping probabilities, respectively. Most importantly, the MV^{2+} ions, which are electrostatically attracted to the trapped Cl^- ions, are therefore reduced to less than ~100 ions for the 0.90 trapping probability case, and essentially shut down (<50 ions) for the 0.95 trapping probability case. The more mobile ion determines the fate of the less mobile ion.

Coating the membrane with gold effectively removes the charge on the surface of the membrane and at least partially, if not completely, throughout the membrane pores. Such coating was found to significantly reduce, but not totally eliminate the gating, consistent with evidence that the mobile ion is attracted and trapped by the oppositely charged membrane. These experimental results furthermore suggest that the gold covered and masked the top region of the pore where the electric field is greatest (see Fig. 3) rather than necessarily completely covering the entire length of the pore. Such a geometry is expected when depositing a metal by sputtering.

When 100 mM KCl is added to the feed, the gating effect is also significantly reduced. Here, the salt gives rise to the formation of a Gouy-Chapman double layer of thickness ~0.9 nm which screens the positive charge on the membrane at pH =2, making it less attractive to the chloride ions; the addition of salt acts, in this way, much like the coating with gold discussed above. In the absence of any other effects, the ions would be expected to diffuse through the pore as though it were uncharged. However, the addition of salt also screens the methyl viologen-chloride electrostatic interactions, the Cl^- is no

longer able to bind the MV^{+2}, effectively allowing each ion to diffuse independently. The system is still driven by the more mobile ion in the sense that the Cl^- ion will come through the membrane first but without dragging the MV^{+2} with it.

When the pH is changed to 5, the membrane becomes negatively charged, according to zeta potential measurements.[17,18] If membrane charge was accounting for the gating, we would expect to see the MV^{2+} trapping to the membrane. Instead, we observe both MV^{2+} and Cl^- diffusing through the 100 nm pore, consistent with the mobile ion (Cl^-) diffusing faster and pulling the MV^{2+} through the pore. Since the membrane is negatively charged, the chloride is repelled from a pore wall when in its near proximity (the electric field diminishes rapidly with distance from the pore wall); because the Cl^- diffuses faster than the MV^{2+} and the charges do not separate, the MV^{2+} is effectively pulled through the membrane by the more mobile species, chloride.

The results obtained with $(Na^+)_2$-NDS^{2-} were electrostatically opposite to those observed for the methyl viologen; that is, gating of NDS^{2-} was observed at pH=5 (negatively charged membrane) and diffusion of NDS^{2-} through the membrane occurred at pH=2 (positively charged membrane). Again, these NDS^{2-} experimental observations are consistent with the mobile ion, in this case sodium, driving the system. At pH 5, the Na^+ ions trap to the walls and hold back the slower NDS^{2-}; at pH=2, the Na^+ ions pull the NDS^{2-} molecules through the pore, thus preventing the negative molecules from binding to the positively charged membrane.

Conclusion

It remains to identify possible trapping mechanisms for the more mobile species to the polycarbonate surface. Given that both Cl^- and Na^+ trap to this surface, a chemical

reaction mechanism is unlikely; van der Waals effects might provide the fundamental binding forces.

Our observations of the gating of ionic species in pores much larger than those for which gating was previously reported opens up new opportunities in the field of membrane separation. In particular, greater fluxes can be achieved when pore sizes are larger than those for which double layer overlap provides cation or anion selectivity (generally less than 10 nm). Although in our tests a change in solution pH was used to switch the sign of surface charge from positive to negative, such a change could be induced externally by metalizing the membrane surface and directly applying the desired charge. When used in conjunction with an external field, this technology could separate or collect large charged macromolecules as well as bio-organisms. Potential applications include pre-treatment of waters for desalination, virus removal, drug separation, protein and cell manipulations, and sample pre-concentration for chemical and biological detection.

Acknowledgement. This work was performed under the auspices of the U.S. Department of Energy by University of California Lawrence Livermore National Laboratory under contract W-7405-Eng-48.

References

(1) Toyoshima, C.; Nomura, H.; Tsuda, T. *Nature* **2004**, *432*, 361-368.
(2) Yu, S.; Bok Lee, S.; Kang, M.; Martin, C. R. *Nano Letters* **2001**, *1*, 495-498.
(3) Bok Lee, S.; Martin, C. R. *Anal. Chem.* **2001**, *73*, 768-775.
(4) Martin, C. R.; Nishizawa, M.; Jirage, K. B.; Kang, B.-G. *J. Phys. Chem. B* **2001**, *105*, 1925-1934.
(5) Martin, C. R.; Nishizawa, M.; Jirage, K. B.; Kang, M.; Bok Lee, S. *Adv. Mater.* **2001**, *13*, 1351-1362.
(6) Bok Lee, S.; Martin, C. R. *Chem. Mater.* **2001**, *13*, 3236-3244.
(7) Jirage, K. B.; Hulteen, J. C.; Martin, C. R. *Science* **1997**, *278*, 655-658.
(8) Jirage, K. B.; Hulteen, J. C.; Martin, C. R. *Anal. Chem.* **1999**, *71*, 4913-4918.
(9) Chun, K.-Y.; Stroeve, P. *Langmuir* **2002**, *18*, 4653-4658.
(10) Sanchez-Quesada, J.; Isler, M. P.; Ghadiri, M. R. *J. Am. Chem. Soc.* **2002**, *124*, 10004-10005.
(11) Lee, S. B.; Mitchell, D. T.; Lacramioara, T.; Nevanen, T. K.; Soderlund, H.; Martin, C. R. *Science* **2002**, *296*, 2198-2200.
(12) Siwy, Z.; Fulinski, A. *Phys. Rev. Lett.* **2002**, *89*, 198103-198106.
(13) Siwy, Z.; Kosinska, I. D.; Fulinski, A.; Martin, C. R. *Phys. Rev. Lett.* **2005**, *94*, 48102.
(14) Siwy, Z.; Heins, E.; Harrell, C. C.; Kohli, P.; Martin, C. R. *J. Am. Chem. Soc.* **2004**, *126*, 10850-10851.
(15) Schaldach, C. M.; Bourcier, W. L.; Paul, P. H.; Wilson, W. D. *J. Colloid Interface Sci.* **2004,** *275,* 601-611.
(16) Israelachvili, J. N. *Intermolecular and Surface Forces*, London: Academic Press, **1992**.
(17) Chun, M.-S.; Cho, H. I.; Song, I. K. *Desalination* **2002**, *148*, 363-367.
(18) Huisman, I. H.; Pradanos, P.; Calvo, J. I.; Hernadez, A. *J. Membrane Sci.*, **2000,** *178*, 79-92.

Table of content

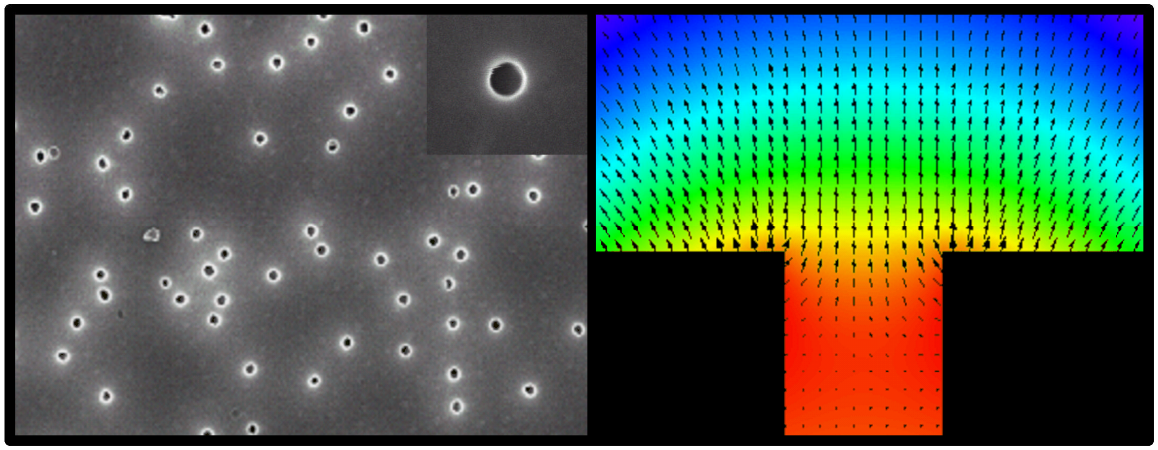

Potential and electric field in the vicinity of the mouth of a 100 nm pore.